\



An extended smart driver model considering electronicthrottle angle changes with memory

Congzhi Wu(武聪智), Hongxia Ge(葛红霞), and Rongjun Cheng(程荣军)
Citation: Chin. Phys. B, 2022, 31 (**1**): 010504. DOI: 10.1088/1674-1056/ac0eec
Journal homepage: http://cpb.iphy.ac.cn; http://iopscience.iop.org/cpb

What follows is a list of articles you may be interested in

Stabilization strategy of a car-following model with multiple time delays of the drivers

Weilin Ren(任卫林), Rongjun Cheng(程荣军), and Hongxia Ge(葛红霞)
Chin. Phys. B, 2021, 30 (**12**): 120506. DOI: 10.1088/1674-1056/abfcc9

Collective motion of polar active particles on a sphere

Yi Chen(陈奕), Jun Huang(黄竣), Fan-Hua Meng(孟繁华), Teng-Chao Li(李腾超), and Bao-Quan Ai(艾保全)
Chin. Phys. B, 2021, 30 (**10**): 100510. DOI: 10.1088/1674-1056/abfccf

Heterogeneous traffic flow modeling with drivers' timid and aggressive characteristics

Cong Zhai(翟聪), Weitiao Wu(巫威眺), and Songwen Luo(罗淞文)
Chin. Phys. B, 2021, 30 (**10**): 100507. DOI: 10.1088/1674-1056/abf7ae

Lagrangian analysis of the formation and mass transport of compressible vortex rings generated by a shock tube

Haiyan Lin(林海燕), Yang Xiang(向阳, Hong Liu(刘洪), and Bin Zhang(张斌)
Chin. Phys. B, 2021, 30 (**3**): 030501. DOI: 10.1088/1674-1056/abc67f

Solid angle car following model

Dongfang Ma(马东方), Yueyi Han(韩月一), Sheng Jin(金盛)
Chin. Phys. B, 2020, 29 (**6**): 060504. DOI: 10.1088/1674-1056/ab862c

---

An extended smart driver model considering electronic throttle angle changes with memory

Congzhi Wu(武聪智)[1,2,3], Hongxia Ge(葛红霞)[1,2,3,†], and Rongjun Cheng(程荣军)[1,2,3]

[1] *Faculty of Maritime and Transportation, Ningbo University, Ningbo* 315211, *China*
[2] *Jiangsu Province Collaborative Innovation Center for Modern Urban Traffic Technologies, Nanjing* 210096, *China*
[3] *National Traffic Management Engineering and Technology Research Centre Ningbo University Sub-centre, Ningbo* 315211, *China*

(Received 26 March 2021; revised manuscript received 6 June 2021; accepted manuscript online 28 June 2021)

Based on the fact that the electronic throttle angle effect performs well in the traditional car following model, this paper attempts to introduce the electronic throttle angle into the smart driver model (SDM) as an acceleration feedback control term, and establish an extended smart driver model considering electronic throttle angle changes with memory (ETSDM). In order to show the practicability of the extended model, the next generation simulation (NGSIM) data was used to calibrate and evaluate the extended model and the smart driver model. The calibration results show that, compared with SDM, the simulation value based on the ETSDM is better fitted with the measured data, that is, the extended model can describe the actual traffic situation more accurately. Then, the linear stability analysis of ETSDM was carried out theoretically, and the stability condition was derived. In addition, numerical simulations were explored to show the influence of the electronic throttle angle changes with memory and the driver sensitivity on the stability of traffic flow. The numerical results show that the feedback control term of electronic throttle angle changes with memory can enhance the stability of traffic flow, which shows the feasibility and superiority of the proposed model to a certain extent.

Keywords: smart driver model (SDM), electronic throttle angle changes with memory (ETSDM), parameter calibration, stability analysis

PACS: 05.60.–k, 45.70.Vn

DOI: 10.1088/1674-1056/ac0eec

1. Introduction

The popularization of motor vehicle not only facilitates people's travel, but also improves the work efficiency. However, as the number of motor vehicle increases year by year, the traffic problems caused by them have become increasingly serious. In order to fundamentally solve the problem of the traffic congestion, some scholars have studied the formation mechanism and evolution law of the traffic congestion.[1–5]

To find out the root cause of the traffic congestion, it is necessary to analyze the dynamic changes of each car in detail. Therefore, some scholars have carried out research on the speed changes and car-following methods of adjacent vehicles.[6–12] Li *et al.*[8] combined the opening angle of the electronic throttle on the basis of the full velocity difference model, so that the proposed model can effectively and quickly eliminate the external disturbances. Zhai *et al.*[12] put forward a car-following model considering electronic throttle, which reveals that the electronic throttle opening angle effect has a considerable impact on the stability of traffic flow. Meanwhile, it is also very important to analyze the overall evolution of traffic flow from a macro perspective.[13–19] Qin *et al.*[13] discussed the effect of electronic throttle on the stability of mixed traffic flow. Jiao *et al.*[14] proposed a new macro model, which contains electronic throttle (ET) and ramp factors. The results indicated that the ET effect play an important role in alleviating traffic congestion to a certain extent.

In 2000, Treiber *et al.*[20] proposed an intelligent driver model (IDM), which can describe the phase transition from free flow to the congested flow in a unified form. IDM provides a new way to solve the problem of traffic congestion, and many scholars have developed new research on traffic problems based on it.[21–24] Subsequently, in order to alleviate the traffic congestion caused by the influx of vehicles, Treiber *et al.*[25,26] optimized the IDM and modified the situation that the actual velocity exceeded the expected velocity. Liu *et al.*[27] discussed the different car following combinations in heterogeneous traffic flow on the basis of IDM, and conducted NGSIM data calibration and simulation experiments on the extended model. Qin *et al.*[28] proposed an extended IDM by using the electronic throttle as a feedback item of IDM, and the results show that the extended model can improve the safety and traffic efficiency.

Milanes *et al.*[29] pointed out that IDM model can produce smooth following behavior, but the response is very slow and the gap changes greatly, which leads to the subsequent vehicle response instability. To address these issues, Lu *et al.*[30] built the smart driver model (SDM), which can make timely adjustment according to the speed difference and headway between vehicles. In addition, SDM provides smoother deceleration and acceleration than IDM.

As one of the four elements of traffic, drivers play an important role in the actual traffic. Due to the difference of driver's technology, reaction speed, physical fitness and other

†Corresponding author. E-mail: gehongxia@nbu.edu.cn

© 2022 Chinese Physical Society and IOP Publishing Ltd

factors, the decision-making also directly affects the stability of traffic flow. Sharma *et al.*[31] introduced the driver's compliance behavior into the vehicle driving strategy, and studied the influence of the driver's compliance on the stability of traffic flow. Yu *et al.*[32] proposed an improved car following model considering the memory changes of multiple vehicle gaps, and concluded that the driver's memory can improve the safety and stability of road traffic flow.

The above research literature shows that whether the micro model or the macro model, using electronic throttle as the feedback control term to improve the model can effectively improve the anti-interference ability of traffic flow and improve the stability of traffic flow. At the same time, although SDM has smooth acceleration and deceleration, it does not consider the driver factor. Can the electronic throttle angle changes with memory as a feedback term be introduced into SDM? How does the angle of electronic throttle change with the driver's memory affect the traffic flow stability? This series of problems need to be further explored and resolved. Therefore, from the perspective of human-vehicle integration, this paper establishes an extended model considering electronic throttle angle changes with memory, and tries to explore the angle of electronic throttle change with the memory on the stability of traffic flow.

The rest of the paper is structured as follows. Section 2 firstly introduces the proposed model, and then the next generation simulation (NGSIM) vehicle trajectory data is applied to calibrate and evaluate the proposed model. In Section 3, we use the method of linear analysis to analyze the new model. In Section 4, numerical simulation is carried out to study the evolution characteristics of traffic flow in the extended model. The final conclusion is given in Section 5.

2. Model description

2.1. The representation of the ETSDM

On the basis of the Gipps model,[33] Treiber *et al.*[20] proposed an intelligent driver model (IDM) considering different congestion dynamics. The IDM essentially defined an acceleration target command generated by the following function:

$$\frac{\mathrm{d}v_n(t)}{\mathrm{d}t} = a\left[1-\left(\frac{v_n(t)}{v_0}\right)^4-\left(\frac{s^*(v_n(t),\Delta v_n(t))}{\Delta x_n - l_n}\right)^2\right], \quad (1)$$

$$s^*(v_n(t),\Delta v_n(t)) = s_0 + \max\left(0, Tv_n(t)+\frac{v_n(t)\Delta v_n(t)}{2\sqrt{ab}}\right), \quad (2)$$

where a is the maximum acceleration, v_0 indicates the desired velocity in free-flow traffic conditions, l_n is the length of the nth vehicle, s_0 represents the static safety distance, T is safe headway, and the desired deceleration is expressed as b.

Lu *et al.*[30] proposed an improved IDM named as SDM, which optimizes the problem of large feedback delay in the car following

$$\frac{\mathrm{d}v_n(t)}{\mathrm{d}t} = a\left[1-\left(\frac{v_n(t)}{v_0}\right)^4\right] - \frac{a\left[1-\left(\frac{v_n(t)}{v_0}\right)^4\right]+\frac{v_n^2-v_{n-1}^2}{2\Delta x}}{\exp\left(\frac{\Delta x}{s_0+v_n\times T}-1\right)}. \quad (3)$$

In this paper, the driver's sensitivity and memory time step are added into the electronic throttle, and a more realistic acceleration model framework is proposed, which is named as smart driver model considering electronic throttle angle changes with memory (ETSDM)

$$\frac{\mathrm{d}v_n(t)}{\mathrm{d}t} = a\left[1-\left(\frac{v_n(t)}{v_0}\right)^4\right] - \frac{a\left[1-\left(\frac{v_n(t)}{v_0}\right)^4\right]+\frac{v_n^2-v_{n-1}^2}{2\Delta x}}{\exp\left(\frac{\Delta x}{s_0+v_n\times T}-1\right)} + \kappa\left(\left(\theta_n(t)-\theta_n(t-\delta)\right)\right), \quad (4)$$

where $\theta_n(t)$ and $\theta_n(t-\delta)$ refer to the angle of the electronic throttle at time t and $t-\delta$, δ denotes the memory step, and κ is the driver's sensitive coefficient.

Ioannou *et al.*[34] proposed that the opening angle of electronic throttle has the following relationship with the vehicle speed and acceleration

$$\frac{\mathrm{d}v_n(t)}{\mathrm{d}t} = -\beta\left(v_n(t)-v_\theta^0\right)+\omega\overline{\theta}_n+e_n, \quad (5)$$

which can be simplified to give

$$\theta_n(t)-\theta_n(t-\delta) = \frac{1}{\omega}\left[\frac{\mathrm{d}v_n(t)}{\mathrm{d}t}-\frac{\mathrm{d}v_n(t-\sigma)}{\mathrm{d}t}+\beta\left(v_n(t)-v_n(t-\delta)\right)\right], \quad (6)$$

where v_θ^0 is the speed when the electronic throttle angle is 0, and β and ω are parameters changing with v_θ^0.

After further derivation and consolidation, we can get

$$\frac{\mathrm{d}v_n(t)}{\mathrm{d}t} = f(v_n(t),s_n(t),\Delta v_n(t)) = \frac{a\left[1-\left(\frac{v_n(t)}{v_0}\right)^4\right]-\frac{a\left[1-\left(\frac{v_n(t)}{v_0}\right)^4\right]+\frac{v_n^2-v_{n-1}^2}{2\Delta x}}{\exp\left(\frac{\Delta x}{s_0+v_n\times T}-1\right)}+H}{1-\frac{\kappa}{\omega}}, \quad (7)$$

where

$$H = \frac{\kappa}{\omega}\left[-\frac{\mathrm{d}v_n(t-\delta)}{\mathrm{d}t} + \beta\left(v_n(t) - v_n(t-\delta)\right)\right]$$

and $v_n(t-\delta)$ is the speed of v_n at time $t-\delta$.

2.2. Next generation simulation data

Next generation simulation (NGSIM) vehicle trajectory data is used to calibrate and evaluate the ETSDM. Table 1 shows the main data used in this paper. The focus of this paper is on car following behavior, and there will be no overtaking or lane changing phenomenon, but these data include various traffic behaviors. Therefore, in order to ensure the accuracy of the experimental results, we screened out 1467 sets of useful data from 1048576 sets of data for experiments.

Table 1. Description of the main NGSIM data.

Columns number	Name	Description
1	vehicle_ID	vehicle number
2	frame_ID	data frame number
9	v_Length	vehicle length
12	v_Vel	instantaneous vehicle speed
13	v_Acc	vehicle instantaneous acceleration
15	preceding	front vehicle number
16	following	following vehicle number
17	space_headway	space_headway
18	time_headway	time_headway

Table 2. Ranges of parameter.

Parameter	Model	
	SDM	ETSDM
a	[1, 3]	[1, 3]
b	–	–
v_0	[30, 40]	[30, 50]
s_0	[4, 10]	[4, 10]
T	[0.5, 2]	[0.5, 2]
β	–	[0, 1]
κ	–	[0, 1]
ω	–	[1, 2]
δ	–	[0, 1]

The objective function F_{obj} of the optimization model for the genetic algorithm is defined as

$$F_{\mathrm{obj}} = \frac{\sqrt{\frac{1}{N}\sum_{1}^{N}\left(\hat{Y}-Y\right)^2}}{\sqrt{\frac{1}{N}\sum_{1}^{N}\left(\hat{Y}^2\right)} + \sqrt{\frac{1}{N}\sum_{1}^{N}\left(Y^2\right)}}, \tag{8}$$

where N represents the sample size, $\hat{Y}$ the actual acceleration, and Y the simulated acceleration of the model.

According to the existing literature, the ranges of parameters in SDM and ETSDM are given in Table 2. The objective function value of the ETSDM is $F_{\mathrm{obj}} = 0.5631$ while the objective function value of the SDM is $F_{\mathrm{obj}} = 0.6235$. Figure 1 illustrates the comparison between computational accelerations of the two models and 1467 sets of real acceleration data for calibration. The blue solid line represents the actual acceleration value, and the red solid line and the green solid line represent the acceleration value simulated by SDM and ETSDM, respectively. According to the comparison by using the verification data, we observe that the improved model shows better fitness with the verification data.

Table 3. The parameter calibration results of models.

Parameter	Model	
	SDM	ETSDM
a	1	1.13
b	–	–
v_0	40	42.6554
s_0	6.736	4.671
T	1.6011	1.4263
β	–	0.16
κ	–	0.4202
ω	–	1.5217
δ	–	0.6143

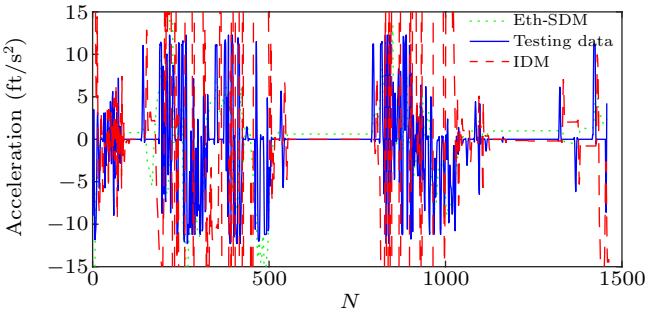


Fig. 1. Comparison of two models with calibration data.

3. Linear stability analysis

The stability of traffic flow mainly studies the evolution process of small disturbance with time in traffic system. The general form of time-continuous car-following models is

$$\frac{\mathrm{d}v_n(t+t_{\mathrm{d}})}{dt} = f\left(v_n(t), s_n(t), \Delta v_n(t)\right), \tag{9}$$

where t_{d} is the time delay, and f is a general nonlinear function.

In addition, Eq. (9) has exactly the same homogeneous flow solution

$$\bar{x}_n(t) = (N-n)\bar{s} + \bar{v}t, \quad n = 1,2,3,\ldots,N, \tag{10}$$

where $\bar{x}_n(t)$ is the location of vehicle n at time t, $\bar{s}$ is the average headway distance between vehicles in a homogeneous traffic flow, and $\bar{v}$ is the velocity of vehicles in homogeneous traffic flow. All of these variables have a definite value in the initial state of traffic flow, in which all vehicles run with the same headway and the same velocity.

Then, $y_n(t)$ denotes the small perturbation from the steady state solution of the vehicle n at time t with the linear

Fourier-mode expanding

$$y_n(t) = ce^{ia_k n+zt} = x_n(t) - \bar{x}_n(t), \quad y_n(t) \to 0, \tag{11}$$

where c is a constant, $a_k = 2\pi k/N$, $(k = 0,1,...,N-1)$, and

$$\begin{aligned} \ddot{y}_n(t+t_\mathrm{d}) &= \ddot{x}_n(t+t_\mathrm{d}) - (\bar{x}_n(t+t_\mathrm{d}))'' \\ &= \ddot{x}_n(t+t_\mathrm{d}) \\ &= \frac{\mathrm{d}v_n(t+t_\mathrm{d})}{\mathrm{d}t}. \end{aligned} \tag{12}$$

Substituting Eq. (9) into Eq. (12), one can obtain

$$\ddot{y}_n(t+t_\mathrm{d}) = f(v_n(t), s_n(t), \Delta v_n(t)). \tag{13}$$

Next, linearizing Eq. (13), we get the following equation:

$$\begin{aligned} \ddot{y}_n(t+t_\mathrm{d}) &= f_s(y_n(t) - y_{n-1}(t)) \\ &\quad + f_{\Delta v}(\dot{y}_n(t) - \dot{y}_{n-1}(t)) \\ &\quad + f_v \dot{y}_n(t), \end{aligned} \tag{14}$$

where $f_v = \frac{\partial f_n}{\partial v_n}\big|_{(\bar{v},\bar{s})} \le 0$, $f_s = \frac{\partial f_n}{\partial s_n}\big|_{(\bar{v},\bar{s})} \ge 0$, and $f_{\Delta v} = \frac{\partial f_n}{\partial \Delta v_n}\big|_{(\bar{v},\bar{s})} \le 0$.

We rewrite Eq. (14) to obtain the difference equation

$$\begin{aligned} \dot{y}_n(t+2t_\mathrm{d}) - \dot{y}_n(t+t_\mathrm{d}) &= t_\mathrm{d} f_s(y_n(t) - y_{n-1}(t)) \\ &\quad + f_v(y_n(t+t_\mathrm{d}) - y_n(t)) \\ &\quad \times f_{\Delta v}(y_n(t+t_\mathrm{d}) - y_n(t) \\ &\quad - y_{n-1}(t+t_\mathrm{d}) + y_{n-1}(t)). \end{aligned} \tag{15}$$

Substituting $y_n(t) = ce^{ia_k n+zt}$ and $\dot{y}_n(t) = zce^{ia_k n+zt}$ into Eq. (15) and simplifying the resulting equation, we get the following equation:

$$\begin{aligned} &(e^{t_\mathrm{d} z} - 1)\left[e^{t_\mathrm{d} z} - f_v - f_{\Delta v}\left(1 - e^{-2ia_k}\right)\right] \\ &= t_\mathrm{d} f_s\left(e^{-ia_k} - 1\right). \end{aligned} \tag{16}$$

Substituting $z = z_1(ia_k) + z_2(ia_k)^2 + \cdots$, and $e^{t_\mathrm{d} z} = 1 + t_\mathrm{d} z + \left[(t_\mathrm{d} z)^2/2\right] + \cdots$, into Eq. (16), we can obtain the first and second order equations for ik,

$$\begin{aligned} z_1 &= \frac{f_s}{f_v}, \\ z_2 &= \frac{\left(1 - \frac{t_\mathrm{d}}{2} f_v\right) z_1^2 - f_{\Delta v} z_1 - \frac{1}{2} f_s}{f_v}. \end{aligned} \tag{17}$$

The homogenous traffic flow is unstable if $z_2 > 0$. On the contrary, when $z_2 > 0$, the homogenous traffic flow is stable. Consequently, the stability condition is given as follows:

$$\frac{1}{2} f_v^2 - f_s + f_v f_{\Delta v} + \frac{t_\mathrm{d}}{2} f_v f_s > 0. \tag{18}$$

In order to draw the neutral stability curve, we find the specific form of f_v, f_s, and $f_{\Delta v}$:

$$\begin{aligned} f_v &= \frac{-\frac{aT}{s_0 + v_\mathrm{e} \times T}\left[1 - \left(\frac{v_\mathrm{e}}{v_0}\right)^4\right] - \frac{8a v_\mathrm{e}^3}{v_0^4} - \frac{\kappa\beta\delta}{\omega}}{1 - \frac{\kappa}{\omega}}, \\ f_s &= \frac{a\left[1 - \left(\frac{v_\mathrm{e}}{v_0}\right)^4\right]}{(s_0 + v_\mathrm{e} \times T)\left(1 - \frac{\kappa}{\omega}\right)}, \\ f_{\Delta v} &= -\frac{v_\mathrm{e}}{(s_0 + v_\mathrm{e} \times T)\left(1 - \frac{\kappa}{\omega}\right)}. \end{aligned} \tag{19}$$

By substituting Eq. (19) into Eq. (18), the stable condition can be further obtained according to the following form:

$$\begin{aligned} \frac{t_\mathrm{d}}{2} < \frac{1}{2} &\frac{\left(\frac{aT}{s_0 + v_\mathrm{e} \times T}\left[1 - \left(\frac{v_\mathrm{e}}{v_0}\right)^4\right] + \frac{8a v_\mathrm{e}^3}{v_0^4} + \frac{\kappa\beta\delta}{\omega}\right)(s_0 + v_\mathrm{e} \times T)}{a\left[1 - \left(\frac{v_\mathrm{e}}{v_0}\right)^4\right]} + \frac{v_\mathrm{e}}{a\left[1 - \left(\frac{v_\mathrm{e}}{v_0}\right)^4\right]} \\ &- \frac{1 - \frac{\kappa}{\omega}}{\frac{aT}{s_0 + v_\mathrm{e} \times T}\left[1 - \left(\frac{v_\mathrm{e}}{v_0}\right)^4\right] + \frac{8a v_\mathrm{e}^3}{v_0^4} + \frac{\kappa\beta\delta}{\omega}}. \end{aligned} \tag{20}$$

We use numerical simulation to draw the neutral stable curve under different conditions. The common parameter values of the two subgraphs in Fig. 2 are as follows: $T = 1.5$ s, $v_0 = 30$ m/s^2, $s_0 = 1.5$ m/s, $\beta = 0.6$ s^{-1}, $\omega = 1.2$ m/s^2·degree^{-1}, and $t_\mathrm{d} = 0$.

Figure 2 illustrates that the area above the neutral stability curve is stable and vice versa. Figure 2(a) shows the neutral stability curve with different parameters $\kappa = 0.1, 0.3, 0.5$, and 0.7. Among these neutral stability curves, it is obvious that the stable region of $\kappa = 0.7$ is larger than that of $\kappa = 0.1$, which means that the stability of traffic flow can be theoretically improved by improving the sensitivity coefficient of the driver's memory. Simultaneously, from Fig. 2(b), we can observe and compare that with the increase of driver memory time step δ, the scope of stability area is increasing, and the stability of traffic flow is enhanced. This implies that the memory time of the driver plays a positive role in the stability of the traffic flow.

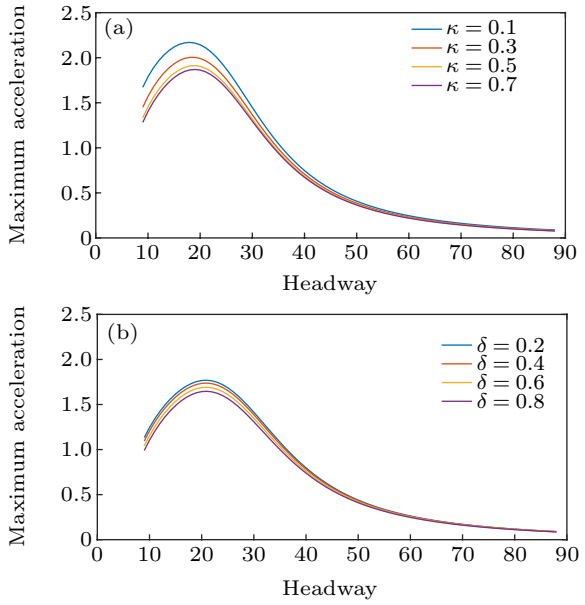


Fig. 2. The headway–maximum acceleration phase diagram with different parameter.

4. Simulation results

This section provides some numerical simulation results to analyze the stability of ETSDM vehicles in different scenarios. Specifically, two cases are considered: (i) the driver's sensitive κ; and (ii) the time step of the driver's memory δ. To facilitate numerical simulation, we discretize Eq. (7) into the following form:

$$v_n(t+\Delta t) = v_n(t) + f(v_n(t), s_n(t), \Delta v_n(t))\Delta t, \quad (21)$$

where Δt is the time step and $\Delta t = 0.1$ s.

We select the following periodic boundary conditions and the initial conditions. The total length of the road is set as $L = 2000$ m and the vehicle length is $l = 5$ m. There will be no overtaking and collision behavior on the road, and the initial speed of all vehicles is0. The parameters selected for simulation are $N = 50$, $a = 1$, $T = 1.8$, $v_0 = 30$, $s_0 = 4$, $\beta = 0.3$, and $\omega = 1.2$. The simulations last for 4000 s with a time step of 0.1 s.

4.1. Driver's sensitivity

This test shows the effect of vehicle speed fluctuating with driver sensitivity. The vehicle is equipped with the ETSDM proposed in the second section, and different driver sensitivity coefficients are simulated to draw correct conclusions. Figure 3 is the space-time evolution diagram of the velocity obtained by adjusting κ equal to 0.1, 0.2, 0.3, and 0.4, respectively. With the help of Fig. 3, one can clearly see how the speed changes. When $\kappa = 0.1$, the response of vehicle speed shows considerable instability, and this fluctuation is amplified downstream, as κ increase, the velocity fluctuation decreases gradually, the vehicle can better follow the speed change of the leading vehicle, and the speed fluctuation is small in the downstream. These results indicate that the driver sensitivity can improve the stability of traffic flow and alleviate traffic congestion. The reason can be analyzed empirically as: drivers with higher sensitivity are more inclined to drive cautiously, and their driving risks are lower than those with lower sensitivity. When the driving status suddenly changes, such as overtaking and emergency stop, the highly sensitive driver can adjust the throttle angle in time to drive the vehicle smoothly.

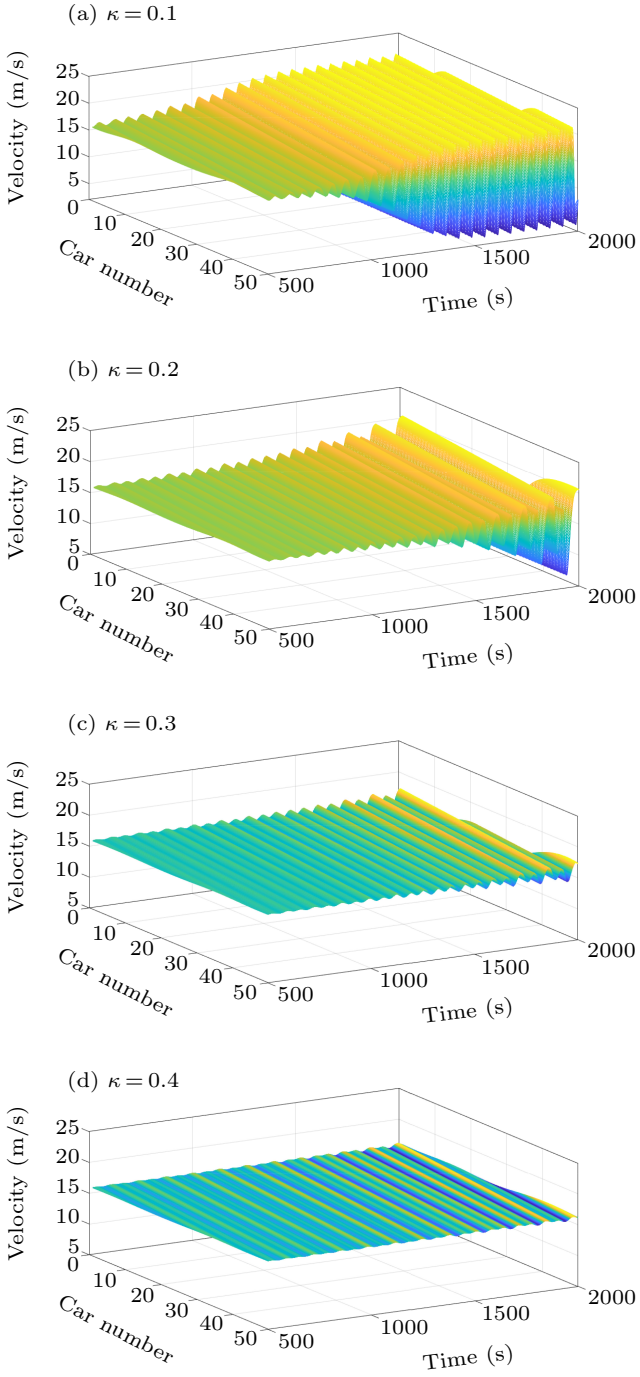


Fig. 3. The space–time evolution of velocity under different values of κ.

Figure 4 is a time-velocity profile diagram corresponding to Fig. 3, and the values of related parameters are consistent

with Fig. 3. By comparing the four pictures in Fig. 4, it is obvious that the smaller the value of κ, the greater the amplitude of the speed fluctuation. The most undesirable behavior appears in Fig. 4(a), starting from the 1000th second, the speed of the vehicle begins to fluctuate significantly, and the downstream turbulence continuesto increase. Meanwhile, the driver's sensitivity is low, and the vehicle cannot be adjusted in time, resulting in great speed fluctuations, which can easily lead to aggressive driving. On the contrary, with the increase of κ, the fluctuation range of speed becomes smaller, and the driving state of the vehicle tends to be stable. Which means that the stability of traffic flow can be theoretically improved by considering the driver sensitivity.

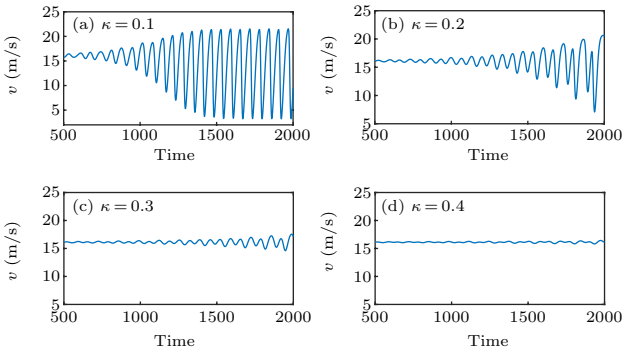


Fig. 4. The velocity profiles for different parameters κ.

4.2. Time step of the driver's memory

Similar to Subsection 4.1, we adopt different δ to explore the relationship between driver's memory time step and traffic flow stability. Figure 5 is the space-time evolution diagram of the velocity obtained by adjusting δ equal to 0, 0.2, 0.4, and 0.6, respectively. In Fig. 5(a), the value of δ is 0, which means that the time step of the driver's memory is not considered. At this time, the traffic flow is very unstable. As shown in Figs. 5(b)–5(d), with δ increases, the amplitude of the velocity wave fluctuations decreases, which indicates that the change of the electronic throttle angle with memory has a positive effect on the stability of traffic flow.

Figure 6 is a two-dimensional velocity evolution diagram corresponding to Fig. 5. From Fig. 6, we can see the change of velocity intuitively. From the 800th second, the speed in Fig. 6(a) fluctuates up and down in the range of 2–22 m/s, and the traffic turbulence is gradually amplified in the downstream. However, with the increase of δ, the amplitude of speed fluctuation decreases rapidly. As can be seen from Fig. 6(d), the speed is basically maintained at 16 m/s, and the oscillation is amplified very little downstream. This is also consistent with our theoretical analysis: the driver's time memory step plays a very positive role in the stability of traffic flow.

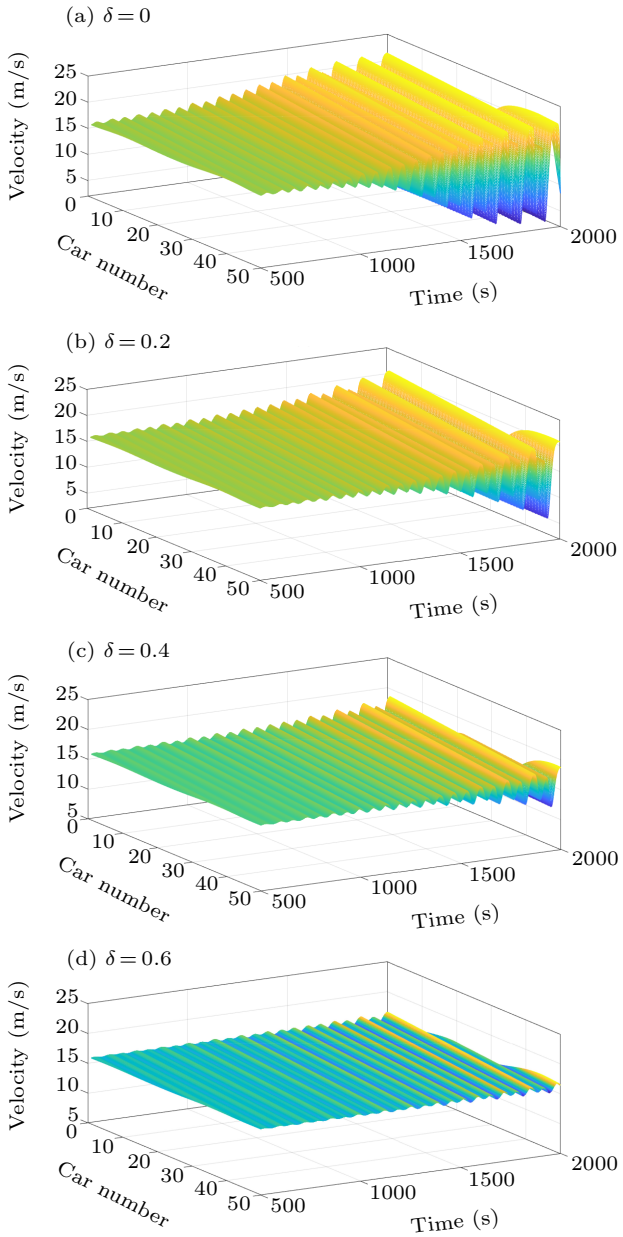


Fig. 5. The space–time evolution of velocity under different values of δ.

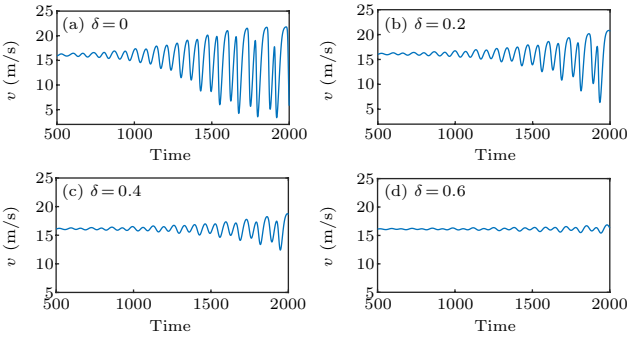


Fig. 6. The velocity profiles for different parameters δ .

5. Concluding remarks

This paper is mainly divided into three parts. Firstly, an extended model is proposed, which uses the change of electronic throttle with memory as a feedback control term.

Then, based on the same group of NGSIM data after screening, this paper uses genetic algorithm to calibrate and evaluate the SDM and ETSDM, respectively. The comparison between the calibration results of the two models shows that ETSDM has a higher degree of fitness.

Secondly, the linear stability analysis method is used to derive the stability conditions of the ETSDM. In order to intuitively analyze the stability region of the model, the neutral stability curve of the model is drawn by using the simulation software. It can be found that the driver sensitivity and time memory step have a positive effect on the stability of traffic flow.

Thirdly, in order to deeply understand the evolution characteristics of traffic flow, we carry out the numerical simulation under periodic boundary conditions, and obtain the spatiotemporal evolution graph of speed. The main conclusions of this paper are as follows:

i. Driver sensitivity plays a positive role in the actual traffic, the higher the sensitivity of the driver, the timelier the adjustment of the vehicle, so as to ensure the smooth and rapid driving of the vehicle.

ii. Considering electronic throttle angle changes with memory can improve the stability of traffic flow.

iii. The results of the numerical simulation are consistent with the theoretical analysis.

Acknowledgments

Project supported by the Natural Science Foundation of Zhejiang Province, China (Grant No. LY20G010004) and the the Program of Humanities and Social Science of Education Ministry of China (Grant No. 20YJA630008), and the K. C. Wong Magna Fund in Ningbo University, China.

References

[1] Bando M, Hasebe K and Nakayama 1995 *Phys. Rev. E* **51** 1035
[2] Newell G F 1961 *Oper. Res.* **9** 209
[3] Pipes L A 1953 *J. Appl. Phys.* **24** 274
[4] Ma C X, Wang H, Pan F Q and Wang X 2018 *PLOS One* **13** e0198931
[5] Zhang Y, Wang S, Pan D B and Zhang G 2021 *Phys. A* **561** 125269
[6] Zhu W X and Li D Z 2018 *Phys. A* **492** 2154
[7] Zhu W X and Zhang H M 2018 *Phys. A* **496** 274
[8] Li F Y, Yang H, Yang B, Zheng T X and Zhang C 2018 *Nolinear Dyn.* **93** 1923
[9] Cao B G 2020 *Phys. A* **539** 122903
[10] Zhu W X and Zhang L D 2016 *Phys. A* **449** 265
[11] Ou H and Tang T Q 2018 *Phys. A* **495** 260
[12] Zhai C and Wu W T 2020 *Eur. Phys. J. B* **93** 52
[13] Qin Y Y and Wang H 2021 *Transport. A-Transport Sci.* **17** 59
[14] Jiao Y L, Cheng R J and Ge H X 2020 *Math. Prob. Engineer.* **2020** 1
[15] Jiang C T, Cheng R J and Ge H X 2019 *Phys. A* **513** 465
[16] Chang Y Y and Cheng R J 2019 *Phys. A* **531** 121751
[17] Cheng R J, Ge H X and Wang J F 2018 *Appl. Math. Comp.* **332** 493
[18] Zhai Q T, Ge H X and Cheng R J 2018 *Phys. A* **490** 774
[19] Cheng R J, Ge H X and Wang J F 2017 *Phys. Lett. A* **381** 2608
[20] Treiber M, Hennecke A and Helbing D 2000 *Phys. Rev. E* **62** 1805
[21] Hook J, Sedky S and Kondoz A 2021 *Cogn. Syst. Res.* **65** 40
[22] Guo L T, Zhao X M, Yu S W, Li X H and Shi Z K 2017 *Phys. A* **471** 436
[23] Moser D, Waschl H, Kirchsteiger H, Schmied R and del Re L 2015 *Control Conference* July 15–17, 2015, Linz, Austria, p. 3383
[24] Zong F, Wang M, Tang M, Li X Y and Zeng M 2021 *IEEE Access* **9** 66241
[25] Kesting A, Treiber M and Helbing D 2010 *Phil. Trans. Royal Soc. A* **368** 4585
[26] Treiber M and Kesting A 2018 *Transport. Res. Part B-Meth.* **117** 613
[27] Liu L, Zhu L L and Yang D 2016 *Appl. Math. Comp.* **273** 706
[28] Qin Y Y, Wang H and Ran B 2018 *IET Intelligent Transport Systems* **12** 921
[29] Milanes V and Shladover S E 2014 *Transport. Res. Part C* **48** 285
[30] Lu C R and Aakre A 2018 *European Transport Research Review* **10** 49
[31] Sharma A, Zheng Z D, Bhaskar A and Haque M M 2019 *Transport.Res. Part B* **126** 256
[32] Yu S W and Shi Z K 2015 *Phys. A* **428** 206
[33] Gipps P G 1981 *Transport. Res. Part B* **15** 105
[34] Ioannou P and Xu T 1994 *IVHS Journal* **1** 413